





# Combined hygrothermal aging and mechanical loading effect on unidirectional glass/epoxy composites

Polymers and Polymer Composites  
Volume 30: 1–10  
© The Author(s) 2022  
Article reuse guidelines:  
[sagepub.com/journals-permissions](https://sagepub.com/journals-permissions)  
DOI: 10.1177/09673911221095261  
[journals.sagepub.com/home/ppc](https://journals.sagepub.com/home/ppc)  


Clarissa C Angrizani<sup>1</sup> , Branca F de Oliveira<sup>2</sup>, Natalia P Lorandi<sup>3</sup>, Heitor L Ornaghi Jr<sup>4</sup>   
and Sandro C Amico<sup>1</sup> 

## Abstract

Composites are subjected to different use conditions. Hence, the mechanical properties under different aging conditions are crucial in the composite field. This study aims to investigate the aging effect of a glass/epoxy unidirectional composite in three distinct conditions: mechanical, hygrothermal (hot water), and combined (mechanical and hygrothermal) aging. The composites in the longitudinal [0°] and transversal [90°] directions were molded by RTM with a 37% volume fraction. The aging effects on tensile, compressive, shear, short-beam properties, and dynamic-mechanical characteristics, in 0° and 90° fiber direction, were studied. The aging conditions are affected differently, depending on the property analyzed. Comparing aged and non-aged composites, the tensile (from 380 GPa to 140 GPa and from 80 GPa to 40 GPa for non-aged and combined aging in 0° and 90° directions, respectively) and compressive strength (from 250 MPa to 50 MPa and from 100 MPa to 25 MPa for non-aged and combined aging in 0° and 90° directions, respectively) showed greater relative drop than the elastic modulus (a decrease of 3–4 GPa for all aging analyzed compared to the no-aged composites) due to a deleterious effect on the interface and the chemical aging present in the polymeric matrix attenuates the deleterious effect on it. Besides, the properties measured in the 0° direction were more affected than in the 90° direction with the combined aging the most affected property.

## Keywords

Resin transfer molding, Combined aging effects, hot water, mechanical loading, unidirectional composite

Received 13 August 2021; accepted 25 March 2022

## Introduction

Polymer matrix composites (PMC) are usually associated with high specific strength and a wide range of properties, depending on the combination of reinforcement/matrix, nature of the constituents, volumetric content, and arrangement of the reinforcement, among others.<sup>1</sup> However, since the composite properties are very dependent on their characteristics, such as type and proportion of constituents as well as the manufacturing conditions,<sup>2</sup> it is difficult to predict and describe a general behavior under certain environmental conditions, as compared to metals, for instance.<sup>3</sup>

The chemical structure of the polymer matrix is particularly sensitive to external factors, modifying the physical, chemical, and especially mechanical properties.<sup>3</sup> The main degradation mechanisms include thermo-oxidative, thermal, and hydrolytic.<sup>4</sup> Hygrothermal aging in PMCs induces various physical and/or chemical effects such as i) plasticization of the matrix by water, hydrolysis of the matrix or molecular degradation with the breaking of polymeric chains, ii) swelling and induced internal stresses, cracking/crazing due to both osmosis and the change in water state; and iii) damage of the fiber/matrix interface and debonding.<sup>5,6</sup>

<sup>1</sup>PPGEM, Federal University of Rio Grande do Sul, Porsto Alegre, Brazil

<sup>2</sup>PGDesign, Federal University of Rio Grande do Sul, Porto Alegre, Brazil

<sup>3</sup>PGMAT, University of Caxias do Sul, Caxias do Sul, Brazil

<sup>4</sup>Department of Materials, Federal University for Latin American Integration (UNILA), Foz do Iguaçu, Brazil

## Corresponding author:

Clarissa C Angrizani, Department of Materials, Federal University of Rio Grande do Sul (UFRGS), Porto Alegre, 90040-060 Av. Bento Gonçalves, 9500 Sector IV, Building 43426, Room 211, Brazil.

Email: [cangrizani@gmail.com](mailto:cangrizani@gmail.com)



Creative Commons Non Commercial CC BY-NC: This article is distributed under the terms of the Creative Commons Attribution-NonCommercial 4.0 License (<https://creativecommons.org/licenses/by-nc/4.0/>) which permits non-commercial use, reproduction and distribution of the work without further permission provided the original work is attributed as specified on the SAGE and Open Access pages (<https://us.sagepub.com/en-us/nam/open-access-at-sage>).

In severe temperature, humidity, and time, hygrothermal aging promotes fiber degradation through dissolution (reduction of strength and stiffness) in addition to the matrix and interface degradation. In glass fiber composites, dissolution consists of the extraction of alkalis from the glass structures.<sup>7</sup> It is important to mention that the factors that may cause the deterioration of a specific product do not act in isolation, i.e., mechanical loading is usually associated with temperature, radiation, and/or fluids exposure.<sup>8</sup> Thus, knowledge of the combined effect of those agents is very important for PMCs in many sectors. The addition of external loading (mechanical) increases the rate, and level of moisture penetration<sup>9</sup> resulting in volume changes.<sup>10</sup> Mechanical degradation mechanisms are irreversible, observable on a macroscopic scale, and include matrix cracking, delamination, interface degradation, fiber breaks and anelastic deformation, with a direct effect on engineering properties such as stiffness and strength.<sup>11</sup> The hygromechanical coupling changes moisture diffusion coefficients and the amount of moisture in the laminas of a laminate. The interlaminar moisture flow is continuous, and the amount of moisture is discontinuous. Basic principles of irreversible thermodynamics can justify this behavior. This effect is explained by the strong coupling between the moisture transport in polymers and the local stress state. Therefore, heterogeneous wetting leads to the absorption/desorption of water and the creation of a multi-scale stress profile (residual mechanical stresses) in a laminate.<sup>9</sup>

Dogan et al.<sup>12</sup> studied the effect of hygrothermal aging and UV radiation on the mechanical behavior of glass/epoxy composites. The authors studied different conditions and a decrease of tensile strength, tensile modulus, absorbed energy, short-beam strength, and the compression-after impact was found for all aging conditions. The exposition of the composites on UV radiation seems to affect more significantly the results obtained, leading to a higher reduction of the properties. In another study, Dogan et al.<sup>13</sup> focused on the glass/epoxy composites coated and the effect of hygrothermal and UV radiation of the gelcoat coloration (black and yellow). The authors claimed a more pronounced decrease of the tensile strength and impact perforation for the black-coated samples in comparison to the yellow one. Wang et al.<sup>14</sup> studied the hydrothermal aging on carbon fiber/epoxy composites with different interfacial bonding strengths and concluded that degradation of the interface was caused by moisture absorption. Surface treatment improved the hydrothermal durability of the composites.

In this context, this work focuses on the investigation of the aging of a unidirectional glass/epoxy composite in hot water under simultaneous mechanical loading compared to isolated mechanical and hygrothermal loadings. The main novelty of the study is to compare the effect of mechanical, hygrothermal, and combined aging in some of the most important mechanical properties in the use of composite materials in the longitudinal and transverse directions. The main findings point out that the properties are affected differently, depending on the test and the direction studied.

## Materials and methods

The materials used to produce the composites were: (i) Unidirectional glass-fiber VEW 090/50 (E-Glass) fabric from Owens Corning (areal density: 450 g/m<sup>2</sup>); (ii) DGEBA (di-glycidyl ether of bisphenol A) epoxy resin (LY 1316) from ARALSUL, and (iii) polyamidoamine hardener (Aradur 450) from ARALSUL. A 100:13 (weight/weight) ratio was used according to the supplier.

Composites were produced by resin transfer molding (RTM) with a fiber volume fraction of 37% according to ASTM D2584 (burning test at 4h/600°C in Sanchis oven). Firstly, the resin + hardener mixture was stirred and degassed in a vacuum oven (at 25°C for 5 min). After, unidirectional glass/epoxy composites (30 × 30 × 0.27 cm) were molded. The RTM was carried out using a positive pressure of 1.34 bar for infiltration, followed by curing at room temperature for 24 h and post-curing in an oven at 60°C for 4 h. It was tested from 2 (DMA) to 5 (other mechanical tests) valid specimens for each test. It was included a representative curve for the DMA test.

In this work, three aging conditions for 15 days (360 h) were studied. For the hygrothermal aging, the samples were cut with an extra length of 10 mm for the orifice. Prior to submersion, the composites were sealed in the transversal area with Epoxy resin. After curing, the samples were subjected to hygrothermal aging in an oven with air circulation at 80°C (Figures 1(a) and (b)) (sealed container to prevent water evaporation) inside an air-circulation oven. For the mechanical aging, the samples were subjected to a constant strain using the apparatus shown in Figure 1(c). Unidirectional 0° or 90° samples were accordingly oriented in that apparatus, being subjected to three-point bending under constant flexural strain (11%) with the aid of three bars perpendicularly aligned in relation to the specimens and controlled displacement of 4 mm at room temperature (this condition is situated in the elastic regime). Finally, some specimens underwent simultaneous hygrothermal aging and mechanical loading by placing the apparatus inside the oven. In this aging condition, it was repeated the mechanical aging requirement, i.e., the mechanical loading (as previously described) was done with the samples immersed in distilled water at 80°C (Figure 1(d)). Samples with and without hygrothermal aging were analyzed using Scanning Electron Microscopy (SEM) to check if any morphological changes occurred in the composite after aging.

After aging, tensile, compression, in-plane shear, and short-beam tests, as well as dynamic mechanical analysis (DMA), were performed on the specimens. The mechanical tests were performed in an Instron 3382 universal testing machine with a 100 kN load cell. Tensile tests were performed according to ASTM D3039, at a speed of 2 mm/min and using clip-extensometers to produce elastic modulus, Poisson's ratio and tensile strength of the composites. Compression tests were carried out according to ASTM D6641 at 1.3 mm/min, and In-plane shear tests according to ASTM D7078 at 2 mm/min. Short-beam tests were performed according to ASTM D2344 using the same equipment but with a 5 kN load cell and at 1 mm/min. And a non-destructive test (ASTM E-1876) was performed using Sonelastic equipment to determine the modulus of elasticity for comparison.

Furthermore, the dynamic mechanical properties of composites were obtained with a DMA Q-800 equipment of TA instruments. The analysis was performed under a single cantilever loading mode, and the conditions were: temperature range

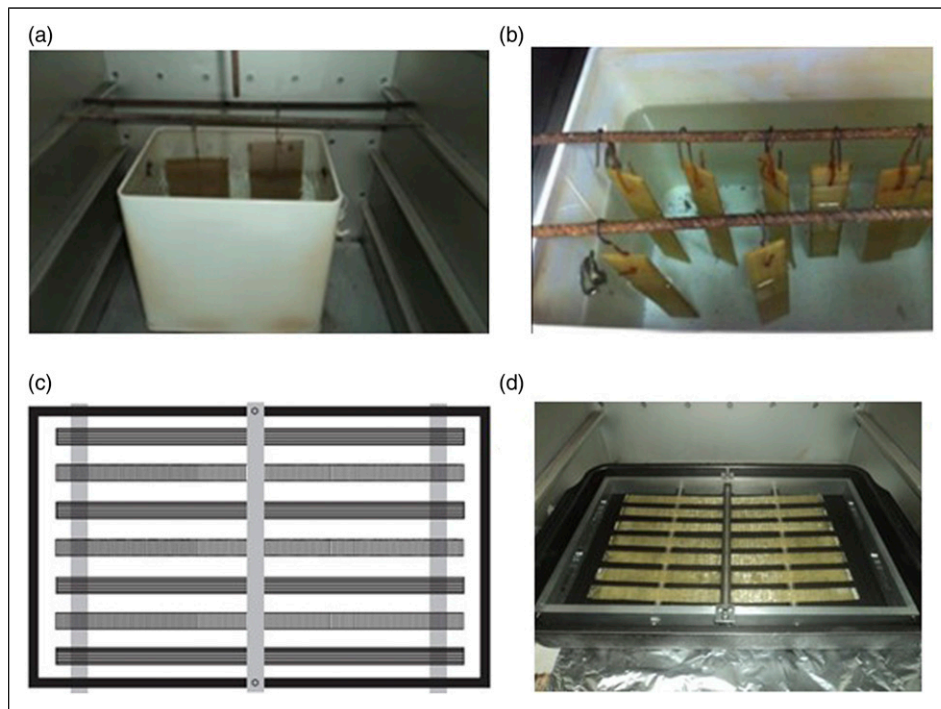


**Figure 1.** Hydrothermal aging for short-beam (a) and tensile tests (b), tensile samples under long-term bending (c), and simultaneous hydrothermal and mechanical loading with the apparatus inside an oven (d).

of 25–150°C, a heating rate of 5 °C/min, a fixed frequency of 1 Hz, and a strain of 0.1%. Theoretical simulated DMA curves were plotted and compared to the experimental ones.

To better assess the reinforcement role in the composite, the reinforcement effect in the composite was estimated as reported in,<sup>15</sup> using the 0° non-aged and 90° non-aged specimens as references. The effectiveness of the reinforcement ( $C_r$ ) was calculated by  $C_r = (E_g/E_r)_{composite}/(E_g/E_r)_{reference}$  where  $E_g$  and  $E_r$  are the glassy and rubbery storage moduli at the chosen temperatures of 30 and 120°C, respectively. According to this equation, the more reinforced materials show comparatively lower  $C_r$  values.

## Results and discussion

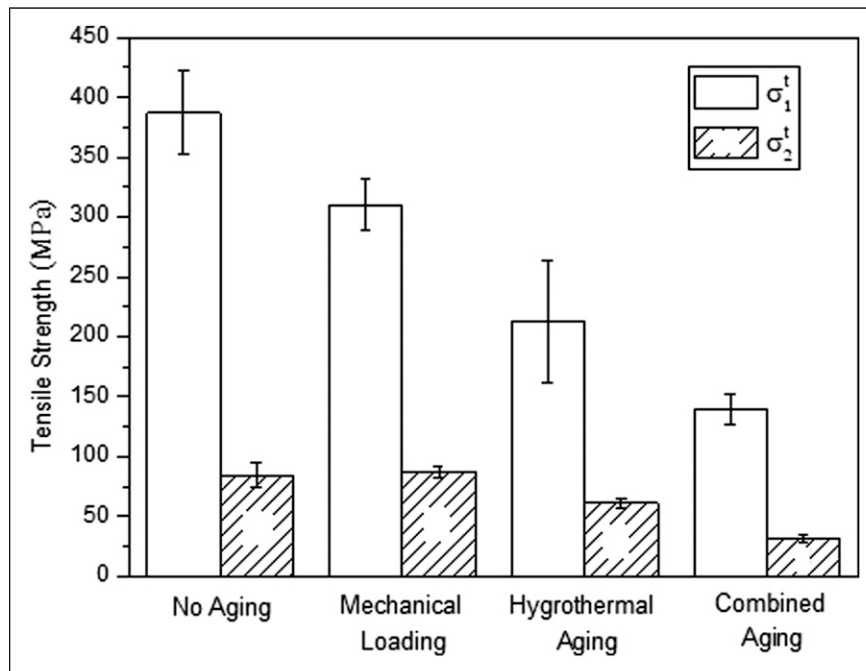
### Tensile strength

Figure 2 shows the mean values of tensile strength of the composites before and after being subjected to mechanical loading and/or hydrothermal aging. Comparing  $\sigma_1^t$  (longitudinal tensile strength) and  $\sigma_2^t$  (transverse tensile strength), it can be observed that, for the three conditions, the relative decrease in  $\sigma_1^t$  is more pronounced, which is attributed to a greater influence of the decay in interfacial characteristics in the former. For the combined aging the decreasing of tensile strength was more pronounced than for the other aging conditions. In the longitudinal direction, a decrease of ~ 37% was noted while in the transverse direction the tensile strength decreases ~50%. The mechanical and hydrothermal aging have a reduction from 380 MPa to 310 MPa and 210 MPa, respectively for  $\sigma_1^t$ . For  $\sigma_2^t$ , there was a decrease from 80 MPa to 60 MPa for the non-aged to the hydrothermal aging. In this condition, the tensile strength for mechanical aging maintains similar values. According to Huang et al.<sup>16</sup> the transported water into the composite deteriorates the interfacial bonding due to the reduction of chemical bonds and mechanical interlocking at the fiber/matrix interface. This effect is better observed in the composite called 0°, whose properties depend mainly on the performance of the fibers.

Also, for the conditions used in this work, hydrothermal aging caused a much greater impact in the composite than the mechanical loading, because the flexural strain was low or the matrix absorbed too much water at 80°C.<sup>17</sup> According to Zhong et al.,<sup>18</sup> epoxy/glass fiber composite hydrothermal aging at 80°C caused swelling of the matrix and cracks near the fiber tows due to differential expansion. Furthermore, an increase in the free volume of the composite due to the tensile stresses under bending for the combined loading allowed an increase in moisture absorption,<sup>19</sup> which resulted in a greater drop in tensile strength compared to the sample subjected to hydrothermal loading only, with greater loss in fiber/matrix adhesion, delamination and microcracking.<sup>20</sup> It is important to notice that the decrease in  $\sigma_1^t$  with the mechanical loading occurred despite being still inside the elastic strain region, so damage may have occurred due to shear stresses or creep.<sup>20</sup> And, this effect was not as pronounced for the 90° sample.

### Microscopy

The micrographs before (Figure 3(a)) and after hydrothermal aging (Figure 3(b)) of the composites show chemical degradation (represented by embossed region in the matrix) characterized by swelling regions. This effect is related to



**Figure 2.** Tensile strength of the composites studied.

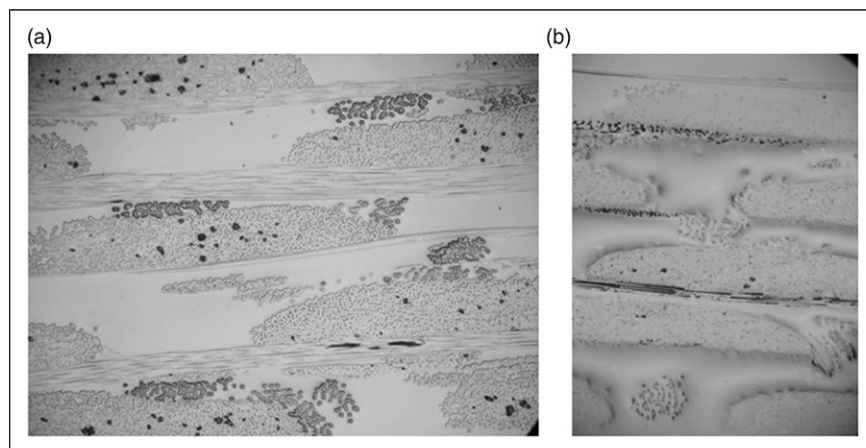


**Figure 3.** 50-fold magnified micrographs of composites before (a) and after hygrothermal aging (b).

matrix hydrolysis that, along with plasticization and loss in fiber/matrix adhesion, tend to reduce their strength and modulus.<sup>21</sup>

### Elastic modulus

Figure 4 shows the mean  $E_1$  and  $E_2$  (longitudinal and transverse elastic modulus) values from tensile and nondestructive testing.  $E_1$  is much higher than  $E_2$ , as expected, and  $E_1$  from the nondestructive testing is slightly higher than that from the tensile testing. For both directions, a decrease from 3 to 4 GPa was observed comparing the non-aged composites (20 GPa and 7 GPa) with mechanical (17 GPa and 5 GPa), hygrothermal (18 GPa and 6 GPa), and combined (16 GPa and 4 GPa) aging. This is in accordance with Divós and Tanaka,<sup>22</sup> who mentioned that it is natural to find values up to 10% higher using a dynamic technique instead of a static technique (tensile test) due to the difference in testing time and strain.

As for the influence of aging, Figure 4(a) and (b) shows a similar trend for  $E_1$  and  $E_2$ . Also, it is interesting to notice that the continuous mechanical loading was more detrimental to the composite stiffness than the hygrothermal aging. This may be also due to damage at the interface resulting from shear stresses<sup>20</sup> that might have caused a flow in the matrix. According to Belec et al.,<sup>23</sup> water is expected to plasticize the epoxy network and lower the modulus due to an increase in free volume and ease of segmental motion when a load is applied to the composite.

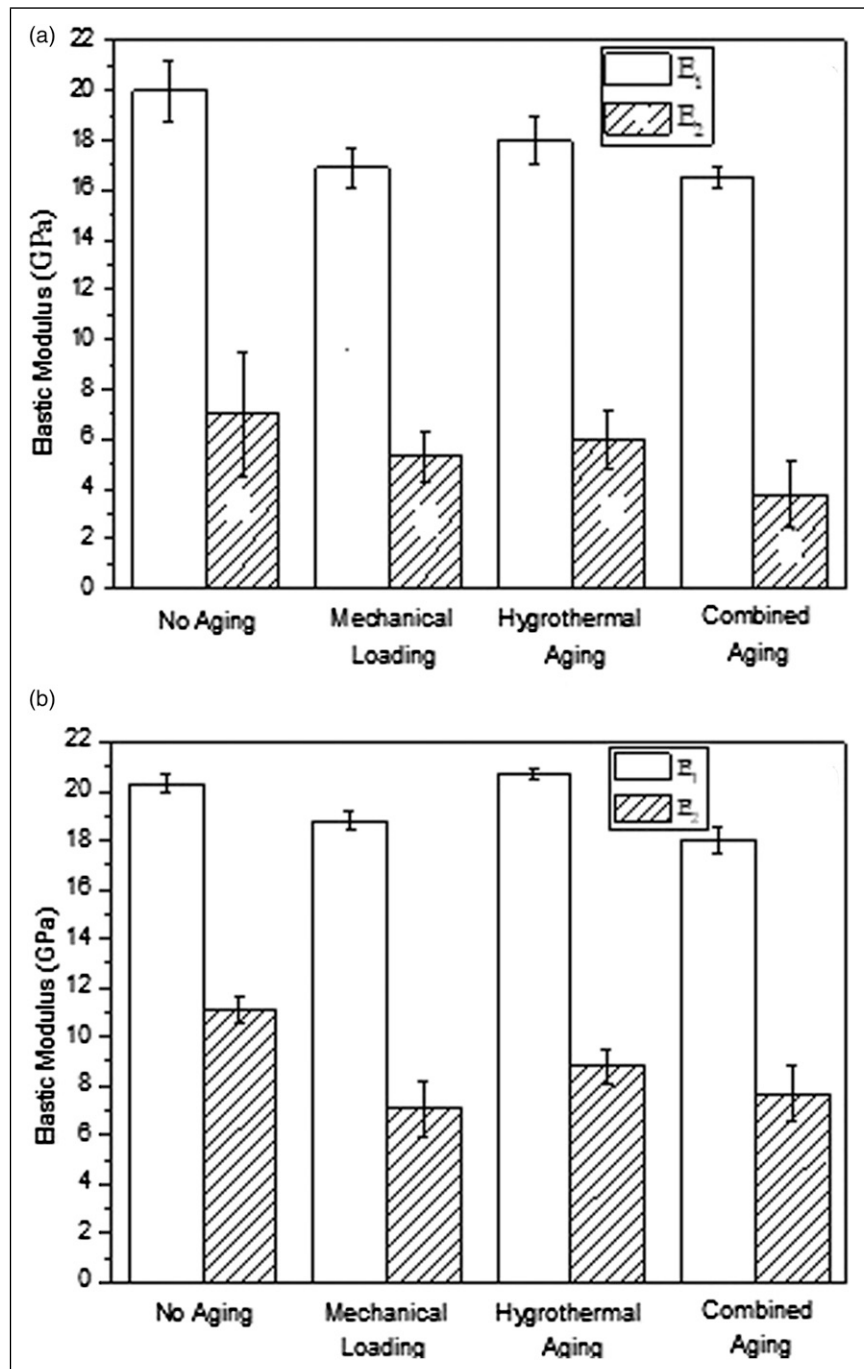


**Figure 4.** Elastic modulus of the composites from tensile (a) and nondestructive (b) testing.

### *In-plane shear strength*

The in-plane shear strength ( $\tau_{12}$ ) of the composites before aging and after mechanical, hydrothermal, and combined aging were  $(38.5 \pm 1.1)^a$ ,  $(45.2 \pm 2.7)^b$ ,  $(37.7 \pm 2.9)^a$  and  $(22.4 \pm 3.6)^c$  MPa, respectively. Despite the water absorption, in the hydrothermal aging, a reduction in this property was not observed, which can be explained by the chemical degradation (Figure 3(b)) of the resin which causes a second cross-linking of the polymeric matrix.<sup>24</sup> In relation to the mechanical loading, it could have influenced the interface, reducing the void content, due to the presence of concentrated force resulting from the use of the apparatus, which would result in an increase in shear strength. Kafodya et al.<sup>25</sup> verified that the combined aging (flexural loading with hydrothermal aging) generated cracks in the matrix between the fibers, loss of fiber/matrix adhesion, and “cleaning” of the surface of the fiber with less adhesion. Therefore, according to these results, it is believed that localized deformation with the bending apparatus, induced microcracks and composite delamination that enhanced water uptake and interfacial degradation.

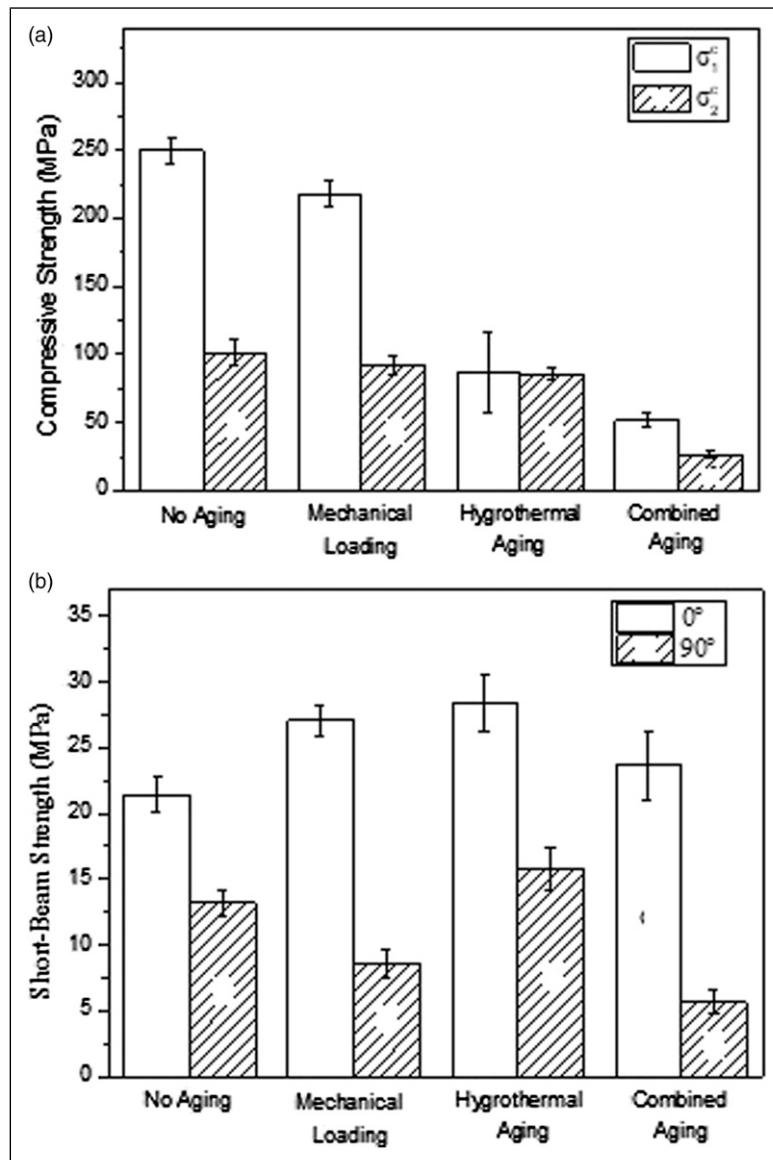


**Figure 5.** Compressive strength (a) and short-beam strength (b) of the composites.

### Compressive and short-beam strength

Figure 5(a) shows the mean values of compressive strength of the composites. The transverse compressive strength ( $\sigma_2^c$ ) did not show a significant decrease, except for the sample submitted to the combined loading, differing from the longitudinal compressive strength ( $\sigma_1^c$ ), which was significantly impacted even with the mechanical loading only. Regarding the mechanical aging for both directions, a decrease of 10% was observed while for the hygrothermal aging the values were reduced by 36% for  $\sigma_1^c$  and 15% for  $\sigma_2^c$ . The combined aging was reduced 5 and fourfold when compared to the non-aged composites for the longitudinal and transverse directions, respectively. According to Helbling and Karbhari,<sup>26</sup> the compressive strength is influenced by residual thermal stresses (due to mismatch in coefficient of thermal expansion between matrix and fiber) as well as cure shrinkage compressive stresses along the fibers during manufacturing of the composites. However, due to moisture-induced swelling, the fiber axial stresses may be reduced and can ultimately change from compression to tension at a critical moisture content that will depend upon the level of pre-existing residual stresses,<sup>27</sup> and this may justify the drop in  $\sigma_1^c$  after hygrothermal aging and combined loading. In relation to the drop in compressive strength after mechanical loading, although the material is in the elastic regime, this could have occurred due to interface damage resulting from shear stresses<sup>28</sup> that may have caused a flow in the matrix reducing the influence of residual stresses. For compressive strength, similarly to tensile strength, the presence of microcracks and loss of matrix/fiber adhesion from the combined loading strongly affected the strength of the aged composite. According to Xian et al.<sup>28</sup> occurs an increase in free volume in the composite due to tensile stresses in the combined loading (hygrothermal environment plus flexure mechanical apparatus) that can allow an increase in moisture inside the composite, which result in a greater drop in compressive strength compared to composite subjected to hygrothermal loading as a result of a higher loss of fiber/matrix adhesion and delamination. According to Helbling and Karbhari,<sup>26</sup> the accumulation of water at hygroscopic sites along the interphase can produce an osmotic pressure that can be sufficient to cause debonding.

Figure 5(b) shows the mean values of the short-beam strength of the composites. In relation to hygrothermal loading, the second crosslinking of the polymeric matrix may be dominant since there was chemical degradation (Figure 3) (the values increase from 22 MPa to 28 MPa for 0° and from 12 MPa to 15 MPa for 90°). The mechanical loading may have influenced the interface, reducing void content, due to the loading that the specimen is subjected to (for 0° the values increase to 27 MPa and for 90° decreases for 7 MPa). In the case of the combined loading, in addition to the above factors, spacing between laminas may increase facilitating the transport of water in the composite, with the appearance of microcracks due to hygroscopic stresses from matrix swelling.<sup>25</sup> This facilitates the entry of water accelerating the loss of property. Kafodya et al.<sup>25</sup> studied this property but found a decrease in strength after aging (for the temperature of 24°C), which may indicate the absence of chemical degradation because it is carried out at low temperatures. For the longitudinal direction, the values were maintained similarly while a reduction of 42% was observed for the transverse direction.

### Dynamic mechanical analysis

Regarding the DMA results, Figure 6(a) and (b) shows the storage modulus and tan delta of the composites. In Figure 6(a), the glassy storage modulus curves follow a similar general trend regardless of aging. Since the change in glassy modulus is a complex function of many influencing factors, it cannot be directly related to the crosslink density or the moisture content. Table 1 shows the  $C$  values for the studied composites and the results suggest that the fibers present the highest reinforcement effect after hygrothermal aging and the lowest after mechanical loading.

In Figure 6(b), the decrease in  $T_g$  indicates plasticization effects with moisture uptake. The height of the tan delta peak gradually decreases with aging, reflecting the effects of slow curing under room conditions and moisture-induced plasticization. Post-curing probably enhanced the crosslink density and reduced mobility of the molecular chains as indicated by the lower energy loss in the transition region. Moisture between molecular segments can also reduce segmental interaction, contributing to that decrease.<sup>29,30</sup>

The peak height of the tan delta maximum is indicative of the interface quality, mainly in the glass transition region.<sup>31</sup> Also, the temperature at which occurs the maximum dissipation energy can be indicative of the reinforcement effect. Table 2 shows the tan delta peak height values for all studied composites based on Figure 6(b). It is clear that a reinforcement effect at room temperature is not necessarily associated with a reinforcement effect in the glass transition temperature (results presented in parenthesis). But the results suggest that mechanical loading affected the interface of the composite, with higher values of dissipation energy. Lower dissipation energy means that the stress transferred to the fibers from the matrix is not dissipated as heat per cycle of deformation, so fibers carry a great portion of the applied stress. Hygrothermal aged samples showed dissipation energy similar to the respective non-aged samples, which means that the interface quality is similar in such cases, i.e., small deleterious effect on the interface under this condition.

The decrease in  $T_g$  values upon the hygrothermal environment is due to resin plasticization and water/resin interaction in the composite,<sup>32</sup> with degradation of the fiber/matrix interface.<sup>33,34</sup> At lower temperatures, the plasticization effect is usually reversible whereas, at elevated temperatures, it can produce irreversible effects due to chemical degradation of the matrix and interface, and an increase in internal voids from chain expansion producing microcracks in the matrix.<sup>34</sup>

The interface strength can be indirectly calculated using the same approach as proposed by Chirayil et al.,<sup>35</sup> which relates that the peak height of the tan  $\delta$  curves is a reflection of constrained regions (Table 3). These constrained regions quantitatively measure the fraction of the composite that contributes to lower dissipation energy as heat for the composites and can be calculated by Equations (1)–(3)

$$W = \frac{\pi \tan \delta}{\pi \tan \delta + 1} \quad (1)$$

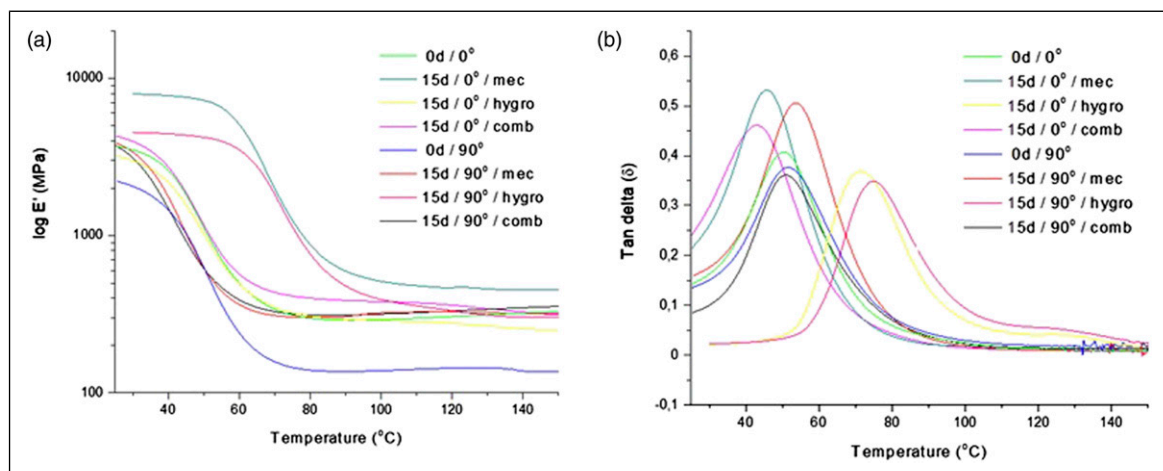


Figure 6. (a) Storage modulus and (b) tan delta dynamic curves for composites exposed to aging.

**Table 1.** Coefficient of reinforcement effectiveness for the studied composites.

0°	$C_r$	90°	$C_r$
Mechanical loading	0.93	Mechanical loading	1.29
Hygrothermal aging	0.79	Hygrothermal aging	0.79
Combined aging	0.84	Combined aging	1.03

\*Non-aging composites were used as reference.

**Table 2.** Tan  $\delta$  peak height maximum and the associated temperature ( $T_g$ , in parenthesis) for the studied composites.

0°	Tan $\delta$ peak height maximum	90°	Tan $\delta$ peak height maximum
No aging	0.41 (50.5°C)	No aging	0.38 (51.9°C)
Mechanical loading	0.53 (45.8°C)	Mechanical loading	0.50 (53.7°C)
Hygrothermal aging	0.42 (42.7°C)	Hygrothermal aging	0.39 (46.5°C)
Combined aging	0.46 (43.2°C)	Combined aging	0.36 (51.3°C)

**Table 3.** Constrained region for the composites studied. The values were compared considering the composites with higher peak height (see Table 2).

0°	Constrained region	90°	Constrained region
No aging	0.23	No aging	0.28
Mechanical loading	—	Mechanical loading	0.06
Hygrothermal aging	0.21	Hygrothermal aging	0.26
Combined aging	0.13	Combined aging	0.32

$$W = \frac{(1 - C) \times W_0}{1 - C_0} \quad (2)$$

$$C = 1 - \frac{(1 - C_0) \times W}{W_0} \quad (3)$$

where  $W$  is the energy loss fraction of the composite at the tan  $\delta$  peak,  $C$  is the volume fraction of the constrained region,  $W_0$  and  $C_0$  are the energy fraction loss and volume fraction of the constrained region of the composite with higher peak height, respectively. Rearranging equation (2) into equation (3), where  $C_0$  is now taken to be zero for the higher peak height composite and the height of the tan  $\delta$  is used to calculate  $W$  according to equation (2).

In the glassy region, there is a minimal or even negative contribution of the stiffness of the fibers to a higher modulus. The values are dependent on the fiber orientation and aging and not on the fiber. With temperature, the abrupt drop of the matrix modulus is compensated by fiber stiffness, which reduces the modulus drop in such a way that it is noticeable only in the elastomeric region. In the glass transition zone, an increase in the free volume is expected because of an increase in molecular motion.<sup>36,37</sup> Since the reinforcement content is the same for all composites, the constrained region will be a reflection of the aging type. Both lower (mechanical loading) and higher (combined aging) constrained regions were obtained for 90° composites. The higher constrained region presented by the combined aging is indicative that this method was less susceptible to plasticization effect on interface compared to the other samples in the glass transition region.

The interfacial strength determines how much of the applied stress can be transferred to the load-bearing fibers and reflects in the energy dissipation peak. The contact area between fibers and matrix and adhesion level at the contact points play a major role in interfacial strength.<sup>34,38,39</sup> The width of the relaxation curve reflects changes in the relaxation time distribution which can cause debonding of fiber/matrix interface during hygrothermal and/or combined aging conditioning. If the interface is affected by aging, modifications in the relaxation mechanism take place, with possible changes in the  $\alpha$ -transition and/or peak height. So, peak dissipation will be reduced by poorer interface adhesion, with a reduction in  $T_g$ . This hypothesis is corroborated by shear strength as well other mechanical properties not dominated by the fiber properties. A schematic representation of the energy dissipation and the influence of the fiber can be found on Ornaghi Jr et al.<sup>40</sup> study.

## Conclusions

In this work, the influence of mechanical loading and hygrothermal aging, isolated or combined, on epoxy/glass unidirectional composites was studied at 0° and 90°. In general, the hygrothermal aging presented a greater influence on the mechanical properties than the mechanical loading, leading to the conclusion that the predominant factors were second matrix crosslinking (which can be inferred by the chemical degradation verified in the SEM) and the loss of fiber/matrix adhesion.



The tensile and compressive strength were the most affected with aging, with a greater reduction for the samples oriented at 0°- a reduction from 380 MPa to 140 MPa for tensile and from 250 MPa to 50 MPa was observed for compressive strength, respectively. For the samples oriented at 90° a reduction from 80 MPa to 0 MPa for tensile and from 100 MPa to 25 MPa for compressive strength was noted. For both orientations, the mechanical aging showed less influence compared to the non-aged composite. For the elasticity modulus properties, this decrease was less significant, due to a greater influence of the second matrix cross-linking. A reduction in an order of 3–4 GPa was observed for all conditions compared to the non-aged composite. A more negative influence of the combined aging was found for the aforementioned tests. The in-plane shear strength showed higher values for the mechanical aging (~45 MPa) compared to the non-aged and hygrothermal aging (38 MPa). Again, the combined aging showed lower values of 22 MPa. The short-beam analysis showed higher values for mechanical (27 MPa), hygrothermal (28 MPa), and combined (23 MPa) compared to the non-aged composite (22 MPa) for the 0°. For the 90° orientation higher values were obtained for the hygrothermal aging (15 MPa) compared to the non-aged (12 MPa), mechanical (7 MPa), and combined (5 MPa). In the dynamic mechanical analysis, the lower difference between the glass and elastomeric states was observed for the hygrothermal aging. Post-curing probably enhanced the crosslinking density, reducing molecular mobility at the glass transition region, shifting the  $T_g$  to higher temperatures. This was corroborated by the lower dissipation energy for the tan delta peak. Also, hygrothermal composites showed a greater reinforcement effect.

Briefly, the aging yielded different effects on distinct properties, and cannot be always estimated by simply adding the isolated mechanical or hygrothermal effects. Therefore, the study of the aging behavior of composite material should simulate the actual service conditions for a more suitable analysis.

### Acknowledgements

The authors would like to thank CAPES and CNPq for the financial support.

### Declaration of conflicting interests

The author(s) declared no potential conflicts of interest with respect to the research, authorship, and/or publication of this article.

### Funding

The author(s) disclosed receipt of the following financial support for the research, authorship, and/or publication of this article: This work was supported by the CNPq and CAPES (01).

### ORCID iDs

Clarissa C Angrizani  <https://orcid.org/0000-0002-6216-9712>

Heitor L Ormaghi  <https://orcid.org/0000-0002-0005-9534>

Sandro C Amico  <https://orcid.org/0000-0003-4873-2238>

### References

1. Angrizani CC, Ormaghi HL Jr, Zattera AJ, et al. Thermal and mechanical investigation of interlaminar glass/curaua hybrid polymer composites. *J Nat Fibers* 2017; 14(2): 271–277.
2. Beura S, Thatoi DN, Chakraverty AP, et al. Impact of the ambience on GFRP composites and role of some inherent factors: a review report. *J Reinf Plast Compos* 2018; 37(8): 533–547.
3. Angrizani CC, Oliveira BF and Amico SC. Evaluation of the durability performance of glass-fiber reinforcement epoxy composites exposed to accelerated hygrothermal ageing. *J Mater Sci Adv Tech* 2015; 11: 31–47.
4. Garg A and Chalak HD. A review on analysis of laminated composite and sandwich structures under hygrothermal conditions. *Thin Wall Struct* 2019; 142: 205–226.
5. Guen-Geffroy AL, Gac P-YL, Habert B, et al. Physical ageing of epoxy in a wet environment: coupling between plasticization and physical ageing. *Polym Degrad Stab* 2019; 168: 1–8.
6. Beura S, Sahoo SR, Thatoi DN, et al. Stability of GFRP composites with varied fractions of reinforcement exposed to ageing processes outdoors. *Polym Polym Compos* 2020; 29(9): 1485–1494.
7. Fergani H, Benedetti MD, Oller CM, et al. Durability and degradation mechanisms of GFRP reinforcement subjected to severe environments and sustained stress. *Constr Build Mater* 2018; 170: 637–648.
8. Alam P, Robert C and Brádaigh CMÓ. Tidal turbine blade composites - A review on the effects of hygrothermal aging on the properties of CFRP. *Compos B Eng* 2018; 149: 248–259.
9. Youssef G, Fréour S and Jacquemin F. Stress-dependent moisture diffusion in composite materials. *J Compos Mater* 2009; 43(15): 1621–1637.
10. Neumann S and Marom G. Free-volume dependent moisture diffusion under stress in composite materials. *J Mater Sci* 1986; 21: 26–30.
11. Martin R. *Ageing of Composites*. 1st ed. Boca Raton, FL: CRC Press, 2008.
12. Dogan A and Arman Y. The effect of hygrothermal aging and UV radiation on the low-velocity impact behavior of the glass fiber-reinforced epoxy composites. *Iran Polym J* 2019; 28: 193–201.

13. Dogan A, Arman Y and Ozdemir O. Experimental investigation of transverse loading on composite panels coated with different gelcoat colors subjected to UV radiation and hygrothermal aging. *Mater Res Express* 2019; 6: 025301.
14. Wang Z, Xian G and Zhao XL. Effects of hydrothermal aging on carbon fibre/epoxy composites with different interfacial bonding strength. *Constr Build Mater* 2018; 161: 634–648.
15. Ornaghi HL Jr, Neves RM, Monticeli FM, et al. Viscoelastic characteristics of carbon fiber-reinforced epoxy filament wound laminates. *Compos Comm* 2020; 21: 100418.
16. Huang S, Fu Q, Yan L, et al. Characterization of interfacial properties between fibre and polymer matrix in composite materials – A critical review. *J Mater Res Technol* 2021; 13: 1441–1484.
17. Rocha IBCM, Raijmaekers S, Nijssen RPL, et al. Hygrothermal ageing behaviour of a glass/epoxy composite used in wind turbine blades. *Compos Struct* 2017; 174: 110–122.
18. Zhong Y, Cheng M, Zhang X, et al. Hygrothermal durability of glass and carbon fiber reinforced composites – A comparative study. *Compos Struct* 2019; 211: 134–143.
19. Abdelmola F and Carlsson LA. State of water in void-free and void-containing epoxy specimens. *J Reinf Plast Compos* 2019; 38(12): 556–566.
20. Kim J-K and Mai Y-W. *Engineered interfaces in fiber reinforced composites*. 1st ed. Amsterdam, Netherlands: Elsevier Science, 1998.
21. Yu Y, Yang X, Wang L, et al. Hygrothermal aging on pultruded carbon fiber/vinyl ester resin composite for sucker rod application. *J Reinf Plast Compos* 2006; 25: 149–160.
22. Divós F and Tanaka T. Effects of creep on modulus of elasticity determination of wood. *J Vib Acoust* 1997; 122(1): 90–92.
23. Belec L, Nguyen TH, Nguyen DL, et al. Comparative effects of humid tropical weathering and artificial ageing on a model composite properties from nano- to macro-scale. *Compos A Appl Sci Manuf* 2015; 68: 235–241.
24. Zhou J and Lucas JP. Hygrothermal effects of epoxy resin. Part I: the nature of water in epoxy. *Polymer* 1999; 40(20): 5505–5512.
25. Kafodya I, Xian G and Li H. Durability study of pultruded CFRP plates immersed in water and seawater under sustained bending: Water uptake and effects on the mechanical properties. *Compos B Eng* 2015; 70: 138–148.
26. Helbling CS and Karbhari VM. Investigation of the sorption and tensile response of pultruded e-glass/vinylester composites subjected to hygrothermal exposure and sustained strain. *J Reinf Plast Compos* 2008; 27(6): 613–638.
27. Mohamed M, Brahma S, Ning H, et al. Development of beneficial residual stresses in glass fiber epoxy composites through fiber prestressing. *J Reinf Plast Compos* 2020; 39(13–14): 487–498.
28. Xian G, Li H and Su X. Effects of immersion and sustained bending on water absorption and thermomechanical properties of ultraviolet cured glass fiber-reinforced acrylate polymer composites. *J Compos Mater* 2012; 47(18): 2275–2285.
29. Odegard GM and Bandyopadhyay A. Physical aging of epoxy polymers and their composites. *J Polym Sci B Polym Phys* 2011; 49(24): 1695–1716.
30. Dao B, Hodgkin JH, Krstina J, et al. Accelerated ageing versus realistic ageing in aerospace composite materials. IV. Hot/wet ageing effects in a low temperature cure epoxy composite. *J Appl Polym Sci* 2007; 106: 4264–4276.
31. Romanzini D, Ornaghi HL Jr, Amico SC, et al. Influence of fiber hybridization on the dynamic mechanical properties of glass/ramic fiber-reinforced polyester composites. *J Reinf Plast Compos* 2012; 31(23): 1652–1661.
32. Zhou J and Lucas JP. Hygrothermal effects of epoxy resin. Part II: variations of glass transition temperature. *Polymer* 1999; 40(20): 5513–5522.
33. Núñez L, Villanueva M, Fraga F, et al. Influence of water absorption on the mechanical properties of a DGEBA (n = 0)/1, 2 DCH epoxy system. *J Appl Polym Sci* 1998; 74(2): 353–358.
34. Thomason JL. The interface region in glass fibre-reinforced epoxy resin composites: 1. Sample preparation, void content and interfacial strength. *Composites* 1995; 26(7): 467–475.
35. Chirayil CJ, Joy J, Mathew L, et al. Nanofibril reinforced unsaturated polyester nanocomposites: Morphology, mechanical and barrier properties, viscoelastic behavior and polymer chain confinement. *Ind Crops Prod* 2014; 56: 246–254.
36. Pothan LA, Thomas S and Groeninckx G. The role of fibre/matrix interactions on the dynamic mechanical properties of chemically modified banana fibre/polyester composites. *Compos A Appl Sci Manuf* 2006; 37: 1260–1269.
37. Vijayan PP, Puglia D, Kenny JM, et al. Effect of organically modified nanoclay on the miscibility, rheology, morphology and properties of epoxy/carboxyl-terminated (butadiene-co- acrylonitrile) blend. *Soft Matter* 2013; 9: 2899–2911.
38. Thomason JL. The interface region in glass fibre-reinforced epoxy resin composites: 2. Water absorption, voids and the interface. *Composites* 1995; 26(7): 477–485.
39. Thomason JL. The interface region in glass fibre-reinforced epoxy resin composites: 3. Characterization of fibre surface coatings and the interphase. *Composites* 1995; 26(7): 487–498.
40. Ornaghi HL Jr, Neves RM, Monticeli FM, et al. Modeling of dynamic mechanical curves of kenaf/polyester composites using surface response methodology. *J Appl Polym Sci* 2021; 139: 52078.